JOURNAL OF CATALYSIS 122, 389–405 (1990)

Optimal Catalyst Activity Distribution in Pellets for Selectivity Maximization in Triangular Nonisothermal Reaction Systems: Application to Cases of Light Olefin Epoxidation

S. PAVLOU AND C. G. VAYENAS[1]

Institute of Chemical Engineering and High Temperature Chemical Processes and Department of Chemical Engineering, University of Patras, GR-26110 Patras, Greece

Received June 12, 1989; revised October 18, 1989

The solution to the general problem of determining the optimal catalyst activity distribution for maximization of global selectivity in flat, cylindrical, or spherical catalyst pellets for parallel, consecutive, or triangular reaction networks in presented. The analysis considers both isothermal and nonisothermal pellets with no external gradients and is applicable to any type of kinetics with arbitrary numbers of chemical species participating in each reaction step. It is shown that the optimal catalyst distribution is an appropriately chosen Dirac δ function. Physically, this implies that the active catalyst must be deposited in a thin zone at a specific distance from the center of the pellet. Analytical expressions are derived for the optimal catalyst location in terms of the pertinent physicochemical and operating parameters. The analysis is applied to C_2H_4 and C_3H_6 epoxidation on Ag. It is shown that pellets with optimal catalyst distribution result in global selectivities that are substantially higher than those obtained with uniformly activated pellets.

INTRODUCTION

The effect of nonuniform activity profiles on the performance of catalyst pellets was first discussed by Shadman-Yazdi and Petersen in 1972 (*1*). The application of nonuniform activity profiles to the commercially important problem of automotive catalyst design has been discussed by Wei and Becker (*2*) and by Hegedus and coworkers (*3–5*). Activity per unit catalyst mass and poisoning resistance were improved by using reaction engineering tools to optimally deposit the catalytic metals within the automotive catalyst pellets. Such work has resulted in a dramatic increase in the service life of automotive catalysts.

Recently, several theoretical studies on the problem of optimal catalyst activity distribution have been published. Varma and co-workers first solved the problem of maximization of global reaction rate, or equivalently effectiveness factor, in pellets with no external temperature gradients for bimolecular Langmuir–Hinshelwood kinetics (*6–8*). More recently, the maximum effectiveness factor problem was solved analytically for the general case of arbitrary kinetics without or with external temperature gradients (*9*, *10*). It was shown that the optimal catalyst distribution is an appropriately chosen Dirac δ function. Simple analytical expressions were obtained for the optimal catalyst zone location z_{opt} in terms of a single dimensionless number Ω (*9*). Similar conclusions were reached for the related optimization problem of active catalyst mass minimization to obtain a given global catalytic rate (*9*). Experimental and theoretical work prior to 1987 has been reviewed recently (*11*, *12*). Recent experimental studies have shown good agreement between theory and experiment for C_2H_4 hydrogenation on Pd/Al_2O_3 (*13*), CO methanation on Ni/Al_2O_3 (*13*), and CO oxidation on Pt (*14*).

Several studies on the effect of nonuni-

[1] To whom correspondence should be addressed.

0021-9517/90 $3.00

form activity distribution on parallel and consecutive reaction selectivity have been conducted by exploring various monoparametric activity distribution profiles (*15–19*). For the case of parallel reactions in pellets used for C_2H_4 epoxidation, selectivity to ethylene oxide was found to increase as the catalyst concentration increased toward the external pellet surface (*17*). For the same system an attempt was made to establish the optimal catalyst profile by assuming the local catalyst selectivity to be constant throughout the pellet, thus rendering the optimization problem one dimensional (*20*). More recently, a numerical search utilizing orthogonal collocation to integrate the mass and energy balance equations was used to maximize product selectivity in nonisothermal first-order consecutive and parallel reaction networks (*21*).

The problem of determining the optimal catalyst profile for selectivity maximization in parallel reactions was recently solved analytically for arbitrary catalytic reaction kinetics in isothermal pellets (*22*). In the same paper the consecutive reaction selectivity maximization problem was solved for arbitrary kinetics of the desirable reaction and positive-order kinetics of the undesirable one. More recently, analytical solutions for the optimal catalyst profile were obtained for selectivity maximization in the cases of parallel (*23*) and consecutive (*24*) reactions in nonisothermal pellets with arbitrary reaction kinetics.

One important limitation of previous rigorous optimization studies (*6–10, 22–24*) is that they strictly refer to reaction systems where each reaction involves a single reactant. Consequently, the results of these studies are not directly applicable to many catalytic systems of technological importance where two or more reactants are involved per reaction. This problem can be overcome only when there is a single limiting reactant per reaction and other reactants are well in excess of the stoichiometric requirement.

In the present work we analyze and solve the problem of determining the optimal catalyst activity profile in isothermal or nonisothermal flat, cyclindrical, or spherical pellets for triangular reaction networks with arbitrary kinetics. As shown in Fig. 1, there is no limitation whatsoever about the number of reactants involved in each reaction step; thus, the above-mentioned limitation of previous studies is eliminated. Analytical expressions are derived for the optimal catalyst profile in terms of the pertinent physicochemical parameters. The results are then applied to two cases of triangular networks of catalytic interest, i.e., epoxidation of C_2H_4 and of C_3H_6 on Ag (*25–33*). In both cases it is shown that by appropriate design of the catalyst pellets one can obtain global selectivities well in excess of those obtained with uniformly activated catalyst pellets.

It is worth noting that the results of this study are also directly applicable to the limiting cases of parallel or consecutive reaction networks without any limitations on the number of reactants involved in each reaction step. These limiting optimal profile results are a generalization of results recently reported by Vayenas and Pavlou (*22–24*) for parallel and consecutive reaction networks involving a single reactant per catalytic reaction.

THEORY

Problem Formulation

We consider the triangular scheme of reactions shown in Fig. 1, which takes place in a catalyst pellet. The rates of the reactions f_1, f_2, f_3 are, in general, functions of the concentrations of all the species $A_1, \ldots, A_m$ and of temperature T. The equations for the steady-state mass balance of the species and the steady-state energy balance are

$$D_{e,i}\frac{1}{x^n}\frac{d}{dx}\left(x^n\frac{dc_i}{dx}\right) = [(a_{i1}-a_{i2})f_1 + (a_{i1}-a_{i3})f_2 + (a_{i2}-a_{i3})f_3]g(x) \quad i = 1, \ldots, m \quad (1)$$

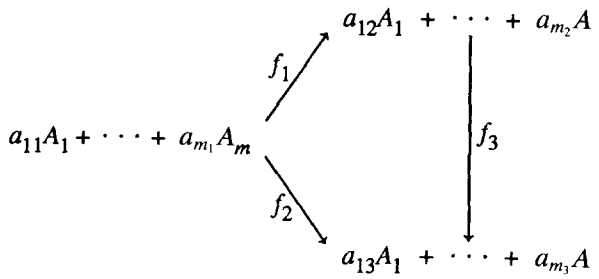

FIG. 1. Triangular reaction network.

$$K_e \frac{1}{x^n}\frac{d}{dx}\left(x^n \frac{dT}{dx}\right) = -[(-\Delta H_1)f_1 + (-\Delta H_2)f_2 + (-\Delta H_3)f_3]g(x). \quad (2)$$

Equation (1) is valid in three cases relevant to this analysis: (i) if the diffusion of all species is in the Knudsen regime; (ii) if the diffusing species can be treated as a pseudobinary system; or (iii) if all the diffusion components are dilute relative to the concentration of a nonreactive species. In Eqs. (1) and (2), $g(x)$ is the local active catalyst density such that

$$\int_{V_p} g(x)dV = g_0 V_p \quad (3)$$

where g_0 is the volume-averaged catalyst density, and $n = 0, 1, 2$ for the infinite slab, infinite cylinder, and sphere, respectively. The boundary conditions of Eqs. (1) and (2) are

$$\frac{dc_i}{dx} = \frac{dT}{dx} = 0; \quad x = 0, \quad i = 1, \ldots, m \quad (4)$$

$$c_i = c_i^0, \; T = T_0; \quad x = R, \quad i = 1, \ldots, m. \quad (5)$$

Introducing the dimensionless quantities

$$z = x/R, \; u_i = c_i D_{e,i}/(c_1^0 D_{e,1}), \; \theta = T/T_0,$$
$$\varphi_j(u_1, \ldots, u_m, \theta) = f_j(c_1, \ldots, c_m, T)/f_j(c_1^0, \ldots, c_1^0, T_0),$$
$$\Phi_j = \{g_0 R^2 f_j(c_1^0, \ldots, c_1^0, T_0)/[(n+1)D_{e,1}c_1^0]\}^{1/2},$$
$$\beta_j = (-\Delta H_j)c_1^0 D_{e,1}/(K_e T_0)$$

and the dimensionless catalyst density $\alpha(z) = g(zR)/g_0$ one can write Eqs. (1) and (2) in the form

$$\frac{1}{z^n}\frac{d}{dz}\left(z^n \frac{du_i}{dz}\right) = (n+1)[(a_{i1} - a_{i2})\Phi_1^2\varphi_1 + (a_{i1} - a_{i3})\Phi_2^2\varphi_2 + (a_{i2} - a_{i3})\Phi_3^2\varphi_3]\alpha(z) \quad i = 1, \ldots, m \quad (6)$$

$$\frac{1}{z^n}\frac{d}{dz}\left(z^n \frac{d\theta}{dz}\right) = -(n+1)(\beta_1\Phi_1^2\varphi_1 + \beta_2\Phi_2^2\varphi_2 + \beta_3\Phi_3^2\varphi_3)\alpha(z) \quad (7)$$

with boundary conditions

$$\frac{du_i}{dz} = \frac{d\theta}{dz} = 0; \quad z = 0, \quad i = 1, \ldots, m \quad (8)$$

$$u_1 = 1, \; u_i = u_i^0, \; \theta = 1; \quad z = 1, \quad i = 2, \ldots, m. \quad (9)$$

From Eq. (3) one has

$$\int_0^1 \alpha(z)z^n dz = \frac{1}{n+1} \quad (10)$$

It should be noted again that in the following analysis, as well as in all previous catalyst profile optimization studies (*6–10, 22–24*), it has been assumed that the effective diffusivities $D_{e,i}$ and the effective thermal conductivity K_e are not dependent on temperature and gaseous composition. This is usually a good approximation, particularly for dilute systems or when Knudsen-type diffusion prevails.

Without loss of generality, one may define A_1 as the key reactant and A_2 as the key

desired product. We consider the case where $a_{11} > a_{12} > a_{13}$ and $a_{22} > a_{21} > a_{23}$, i.e., species A_1 is consumed by all three reactions and species A_2 is produced by reaction 1 and consumed by reactions 2 and 3. Then, the global pellet selectivity is defined as the ratio of the dimensionless net rate of production of species A_2 divided by the stoichiometrically equivalent dimensionless rate of consumption of species A_1:

$$\bar{S} = \frac{-\int_0^1 \left(-\Phi_1^2\varphi_1 + \frac{a_{21}-a_{23}}{a_{22}-a_{21}}\Phi_2^2\varphi_2 + \frac{a_{22}-a_{23}}{a_{22}-a_{21}}\Phi_3^2\varphi_3\right)\alpha(z)z^n dz}{-\int_0^1 \left(\Phi_1^2\varphi_1 + \frac{a_{11}-a_{13}}{a_{11}-a_{12}}\Phi_2^2\varphi_2 + \frac{a_{12}-a_{13}}{a_{11}-a_{12}}\Phi_3^2\varphi_3\right)\alpha(z)z^n dz}. \quad (11)$$

From Eqs. (6), (8), and (11) it follows that

$$\bar{S} = \frac{a_{11}-a_{12}}{a_{22}-a_{21}}\left(-\frac{du_2}{du_1}\right)_{z=1}. \quad (12)$$

The optimal catalyst distribution $\alpha(z)$ is the one which maximizes the objective function $\bar{S}$, as it is defined in Eq. (11) or (12) under the constraint set by Eq. (10) where $u_i(z)$ and $\theta(z)$ can be computed for a given $\alpha(z)$ through Eqs. (6)–(9).

Catalyst Profile Optimization

The optimization problem is substiantially simplified by noting that all the concentrations u_i ($i \geq 3$) can be expressed in terms of u_1 and u_2. Thus, by using Eqs. (6), (8), and (9), one obtains

$$u_i = u_i^o + \frac{(a_{i1}-a_{i3})(a_{21}-a_{22}) - (a_{i1}-a_{i2})(a_{21}-a_{23})}{(a_{11}-a_{12})(a_{21}-a_{23}) - (a_{11}-a_{13})(a_{21}-a_{22})}(1-u_1) + \frac{(a_{i1}-a_{i2})(a_{11}-a_{13}) - (a_{i1}-a_{i3})(a_{11}-a_{12})}{(a_{11}-a_{12})(a_{21}-a_{23}) - (a_{11}-a_{13})(a_{21}-a_{22})}(u_2^o - u_2) \quad i = 3, \ldots, m. \quad (13)$$

Also, from thermodynamic considerations,

$$\beta_3 = \beta_2 - \beta_1. \quad (14)$$

Because of Eq. (14), the dimensionless temperature θ can also be expressed in terms of u_1 and u_2:

$$\theta = 1 + \frac{\beta_1(a_{21}-a_{23}) - \beta_2(a_{21}-a_{22})}{(a_{11}-a_{12})(a_{21}-a_{23}) - (a_{11}-a_{13})(a_{21}-a_{22})}(1-u_1) + \frac{\beta_2(a_{11}-a_{12}) - \beta_1(a_{11}-a_{13})}{(a_{11}-a_{12})(a_{21}-a_{23}) - (a_{11}-a_{13})(a_{21}-a_{22})}(u_2^o - u_2). \quad (15)$$

Then, Eqs. (13) and (15) can be used to eliminate u_i and θ from the rate expressions φ_j and obtain the modified rate expressions $\hat{\varphi}_j$, which are functions of u_1 and u_2 only. Thus, as in the cases of parallel reactions (*23*) and consecutive reactions (*24*), the system can be described by the two differential equations

$$\frac{1}{z^n}\frac{d}{dz}\left(z^n\frac{du_1}{dz}\right) = (n+1)[(a_{11}-a_{12})\Phi_1^2\hat{\varphi}_1(u_1,u_2) + (a_{11}-a_{13})\Phi_2^2\hat{\varphi}_2(u_1,u_2) + (a_{12}-a_{13})\Phi_3^2\varphi_3(u_1,u_2)]\alpha(z) \quad (16)$$

$$\frac{1}{z^n}\frac{d}{dz}\left(z^n\frac{du_2}{dz}\right) = (n+1)[(a_{21}-a_{22})\Phi_1^2\hat{\varphi}_1(u_1,u_2) + (a_{21}-a_{23})\Phi_2^2\hat{\varphi}_2(u_1,u_2) + (a_{22}-a_{23})\Phi_3^2\hat{\varphi}_3(u_1,u_2)]\alpha(z) \quad (17)$$

with boundary conditions

$$\frac{du_1}{dz} = \frac{du_2}{dz} = 0; \quad z = 0 \quad (18)$$

$$u_1 = 1, u_2 = u_2^o; \quad z = 1 \quad (19)$$

By defining the functions

$$h_1(u_1,u_2) = \hat{\varphi}_1(u_1,u_2) + \frac{a_{11}-a_{13}}{a_{11}-a_{12}}\frac{\Phi_2^2}{\Phi_1^2}\hat{\varphi}_2(u_1,u_2) + \frac{a_{12}-a_{13}}{a_{11}-a_{12}}\frac{\Phi_3^2}{\Phi_1^2}\hat{\varphi}_3(u_1,u_2) \quad (20)$$

$$h_2(u_1, u_2) = \left(\frac{a_{11} - a_{13}}{a_{11} - a_{12}} + \frac{a_{21} - a_{23}}{a_{22} - a_{21}}\right) \frac{\Phi_2^2}{\Phi_3^2}\hat{\varphi}_2(u_1, u_2) + \left(\frac{a_{12} - a_{13}}{a_{11} - a_{12}} + \frac{a_{22} - a_{23}}{a_{22} - a_{21}}\right) \frac{\Phi_1^2}{\Phi_3^2}\hat{\varphi}_3(u_1, u_2) \quad (21)$$

Eqs. (16) and (17) can be written in the form

$$\frac{1}{z^n}\frac{d}{dz}\left(z^n \frac{du_1}{dz}\right) = (n + 1)(a_{11} - a_{12}) \Phi_1^2 h_1(u_1, u_2)\alpha(z) \quad (22)$$

$$\frac{1}{z^n}\frac{d}{dz}\left(z^n \frac{du_2}{dz}\right) = (n + 1)(a_{22} - a_{21}) [\Phi_3^2 h_2(u_1, u_2) - \Phi_1^2 h_1(u_1, u_2)]\alpha(z). \quad (23)$$

Because we consider the case where $a_{11} > a_{12} > a_{13}$ and $a_{22} > a_{21} > a_{23}$, the functions defined in Eqs. (20) and (21) are always positive and they can be considered generalized kinetic expressions. Then, Eqs. (22) and (23) have exactly the same form as the equations describing systems of consecutive reactions (*24*). Thus, the same mathematical proof given by Vayenas *et al.* (*24*) can be used to show that the optimal catalyst distribution is a Dirac-type distribution:

$$\alpha(z) = \frac{\delta(z - z_{opt})}{(n + 1)z^n}. \quad (24)$$

That is, all the catalyst must be deposited in a thin zone at a specific distance z_{opt} from the pellet center. The optimal catalyst location z_{opt} is computed from simple expressions which are summarized in Table 1.

As an example, consider the case of linear kinetics in isothermal pellets for the network

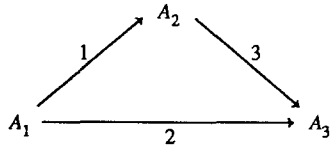

(25)

It is $\varphi_1(u_1, \theta) = u_1 \exp[\gamma_1(1 - 1/\theta)]$, $\varphi_2(u_1, \theta) = u_1 \exp[\gamma_2(1 - 1/\theta)]$, $\varphi_3(u_2, \theta) = \xi u_2 \exp[\gamma_3(1 - 1/\theta)]$, $a_{11} = 1$, $a_{22} = 1$, $a_{33} = 1$, and because $\beta_1 = \beta_2 = \beta_3 = 0$, it follows that $\theta = 1$ and $\varphi_1(u_1) = u_1$, $\varphi_2(u_1) = u_1$, $\varphi_3(u_2) = \xi u_2$. According to Table 1, $u_{1,opt}$ and $u_{2,opt}$ are the u_1, u_2 values which maximize

TABLE 1

Optimal Catalyst Distribution

$$\alpha(z) = \frac{1}{(n + 1)z^n}\delta(z - z_{opt})$$

$$\int_{z_{opt}}^{1} z^{-n}dz = \Omega, \text{ i.e.,}$$

$z_{opt} = 1 - \Omega$ $\quad n = 0$, slab
$z_{opt} = \exp(-\Omega)$ $\quad n = 1$, cylinder
$z_{opt} = 1/(1 + \Omega)$ $\quad n = 2$, sphere

$$\Omega = \frac{1 - u_{1,opt}}{(a_{11} - a_{12})\Phi_1^2\hat{\varphi}_1(u_{1,opt}, u_{2,opt}) + (a_{11} - a_{13})\Phi_2^2\hat{\varphi}_2(u_{1,opt}, u_{2,opt}) + (a_{12} - a_{13})\Phi_3^2\hat{\varphi}_3(u_{1,opt}, u_{2,opt})}$$

$u_{1,opt}$, $u_{2,opt}$: u_1, u_2 values such that $0 \le u_1 \le 1$, $u_i \ge 0$ $(i = 2, \ldots, m)$, which satisfy

$$\frac{u_2^o - u_2}{1 - u_1} = \frac{(a_{21} - a_{22})\Phi_1^2\hat{\varphi}_1(u_1, u_2) + (a_{21} - a_{23})\Phi_2^2\hat{\varphi}_2(u_1, u_2) + (a_{22} - a_{23})\Phi_3^2\hat{\varphi}_3(u_1, u_2)}{(a_{11} - a_{12})\Phi_1^2\hat{\varphi}_1(u_1, u_2) + (a_{11} - a_{13})\Phi_2^2\hat{\varphi}_2(u_1, u_2) + (a_{12} - a_{13})\Phi_3^2\hat{\varphi}_3(u_1, u_2)}$$

and maximize $(a_{11} - a_{12})(u_2 - u_2^o)/[(a_{22} - a_{21})(1 - u_1)]$

Maximum global selectivity: $\bar{S}_{max} = (a_{11} - a_{12})(u_{2,opt} - u_2^o)/[(a_{22} - a_{21})(1 - u_{1,opt})]$

$$\bar{S} = (u_2 - u_2^0)/(1 - u_1) \quad (26)$$

and satisfy

$$(u_2 - u_2^0)/(1 - u_1) = (\Phi_1^2 u_1 - \Phi_3^2 \xi u_2)/[(\Phi_1^2 + \Phi_2^2)u_1]. \quad (27)$$

Defining $\kappa = \Phi_2^2/\Phi_1^2$ and $\lambda = \Phi_3^2/\Phi_1^2$, solving Eq. (27) for u_2, and substituting into Eq. (26) yield

$$\bar{S} = (u_1 - \lambda \xi u_2^0)/[(1 + \kappa)u_1 + \lambda \xi (1 - u_1)]. \quad (28)$$

The parameter $\bar{S}$ is maximized for $u_1 = 1$ when

$$\lambda[1 + u_2^0(1 + \kappa - \lambda \xi)] > 0 \quad (29a)$$

and for $u_1 = 0$ when

$$\lambda[1 + u_2^0(1 + \kappa - \lambda \xi)] < 0 \quad (29b)$$

Consequently, when the kinetic parameters and ambient concentrations satisfy inequality (29a), $u_{1,\text{opt}} = 1$ and, according to Table 1, $\Omega = 0$ and $z_{\text{opt}} = 1$; i.e., the egg shell distribution is optimal. However, when inequality (29b) is satisfield, then $u_{1,\text{opt}} = 0$, $\Omega = 1$, and $z_{\text{opt}} = 0$; i.e., the optimal distribution is of the egg yolk type. Physically, this occurs because when inequality (29b) is satisfied, then λ and u_2^0 are large; i.e., the undesirable reaction $A_2 \rightarrow A_3$ is fast and the ambient concentration of the desired product A_2 is high. Consequently, under such conditions, which could prevail near the exit of a tubular reactor, the optimal policy is to place the catalyst at the pellet center to decelerate the fast undesirable reaction.

Conditions for $z_{\text{opt}} < 1$

The optimal catalyst location z_{opt} depends on the catalytic reaction kinetics and on the heats of reactions and is also affected by the ambient reactant concentrations. In many cases, $z_{\text{opt}} = 1$, i.e., the egg shell catalyst distribution is optimal, but also quite frequently $z_{\text{opt}} = 0$ or $0 < z_{\text{opt}} < 1$, i.e., egg yolk- or egg white-type distributions, respectively, are optimal.

Although Table 1 can readily be used to compute z_{opt} for any triangular reaction network, it is useful to examine under what conditions $z_{\text{opt}} < 1$. Rigorous criteria for $z_{\text{opt}} < 1$ can be derived by the same mathematical procedure described in Refs. (*23*) and (*24*) for the cases of parallel and consecutive reactions. The results are shown in Table 2 for kinetics of the type

$$\varphi_1(u_1, \ldots, u_m, \theta) = \varphi_1^*(u_1) \exp[\gamma_1(1 - 1/\theta)] \quad (30a)$$

$$\varphi_2(u_1, \ldots, u_m, \theta) = \varphi_2^*(u_1) \exp[\gamma_2(1 - 1/\theta)] \quad (30b)$$

$$\varphi_3(u_1, \ldots, u_m, \theta) = \varphi_3^*(u_2) \exp[\gamma_3(1 - 1/\theta)] \quad (30c)$$

TABLE 2

Criterion for $z_{\text{opt}} < 1$: $\Lambda_{\text{cp}} > 0$

Λ_{cp} *definition*
1. For kinetics of the type given by Eq. (30)
$\Lambda_{\text{cp}} \equiv \{\kappa\varphi_2^*(u_2^0)[\gamma_1 - (\lambda + 1)\gamma_2 + \lambda\gamma_3] + \lambda(\gamma_1 - \gamma_3)\}\left[\beta_1 + \beta_2 \frac{\lambda + \kappa\varphi_2^*(u_2^0)}{\lambda + 1}\right]$ $+ \left\{\kappa[\kappa\varphi_2^*(u_2^0) - 1]\left(\frac{d\varphi_2^*}{du_2}\right)_{u_2 = u_2^0} - [\kappa\varphi_2^*(u_2^0)\lambda]\left(\frac{d\varphi_1^*}{du_1}\right)_{u_1 = 1} - \lambda[\kappa\varphi_2^*(u_2^0) - 1]\left(\frac{d\varphi_3^*}{du_1}\right)_{u_1 = 1}\right\}$
2. For linear kinetics
$\Lambda_{\text{cp}} \equiv \{\kappa\xi u_2^0[\gamma_1 - (\lambda + 1)\gamma_2 + \lambda\gamma_3] + \lambda(\gamma_1 - \gamma_2)\}\left(\beta_1 + \beta_2 \frac{\lambda + \kappa\xi u_2^0}{\lambda + 1}\right) + \kappa\xi[u_2^0(\kappa\xi - \lambda - 1) - 1]$

and also for the more special case of linear kinetics, i.e., $\varphi_1^*(u_1) = u_1$, $\varphi_2^*(u_1) = u_1$, and $\varphi_3^*(u_2) = \xi u_2$. These criteria can readily be used to determine whether $z_{opt} < 1$ or $z_{opt} = 1$, but can also be used to gain some physical insight into the effect of the various kinetic and thermodynamic parameters on the optimal catalyst distribution.

As shown in Table 2, a sufficient condition for $z_{opt} < 1$ is $\Lambda_{cp} > 0$. The parameter Λ_{cp} is a generalization of the parameters Λ_p and Λ_c defined in previous publications for parallel (*23*) and consecutive (*24*) reactions, respectively. Although Λ_{cp} appears to be complicated, it contains simple physical information. Both for the case of kinetics described by Eq. (30) and for the more special case of linear kinetics, Λ_{cp} consists of two terms. The first term, which contains the Prater parameters β_j and the Arrhenius parameters γ_j, is a measure of the relative effect of intraparticle temperature gradients on the reaction rates. When this term is positive and large, the rate constant of the desired reaction 1 is increased relative to that of the undesirable reactions 2 and 3 by depositing the catalyst deeper in the pellet. For exothermic reactions ($\beta_j > 0$), this practically happens when the activation energy of the desired reaction is higher than that of the others. As discussed in the next section this happens to be the case for the epoxidation of propylene and is why, for this particular reaction system, usually $z_{opt} < 1$.

The remaining term in Λ_{cp} does not contain the Prater and Arrhenius parameters. It is a measure of the relative intrinsic rates of the three reactions under surface conditions. Consequently, it is also a measure of the relative mass transfer resistance taxation of the three rates when catalyst is deposited inside the pellet. For positive-order kinetics (e.g., linear kinetics) and small ambient concentration of the desired product u_2^0, this term is usually negative. This means that for many cases of practical importance (e.g., linear kinetics) mass transfer resistance considerations dictate that $z_{opt} = 1$. In such cases to have $\Lambda_{cp} > 0$ and $z_{opt} < 1$, there must be a beneficial thermal effect ($\beta_j > 0$, $\gamma_1 > \gamma_2, \gamma_3$) to counterbalance the adverse concentration effect caused by depositing the catalyst deep inside the pellet.

PRACTICAL CONSIDERATIONS

Catalyst Zone Thickness

In the preceding analysis it was shown that Eq. (24) and Table 1 provide the optimal catalyst distribution for selectivity maximization. According to these results, global selectivity is maximized when the active catalyst is deposited in a thin zone located at a distance z_{opt} from the pellet center.

There are, of course, practical considerations, which set a lower limit to the thickness of the active catalyst zone. The main consideration is that of maintaining the active catalyst in a highly dispersed state. This becomes progressively more difficult as the active catalyst zone thickness decreases and as the total active catalyst loading increases. Previous numerical studies (*6*) have shown that when the active catalyst zone thickness is of the order of 4% of the pellet radius, then performance closely approaches the theoretical optimal performance that corresponds to a Dirac δ function. Recent work for the case of single reactions has shown good agreement between experiment and theoretical calculations based on Dirac-type catalyst distributions, even for experimental catalyst zone thicknesses of the order of 10% of the pellet radius (*13*). It is therefore reasonable to expect that the theoretical results presented in the previous section for multiple reaction selectivity maximization can be approximately obtained experimentally.

Experimental Approximation of the Optimal Distribution

Preparation of catalysts with the active ingredient deposited in a thin zone has been discussed by several workers (*1–5, 13, 34,*

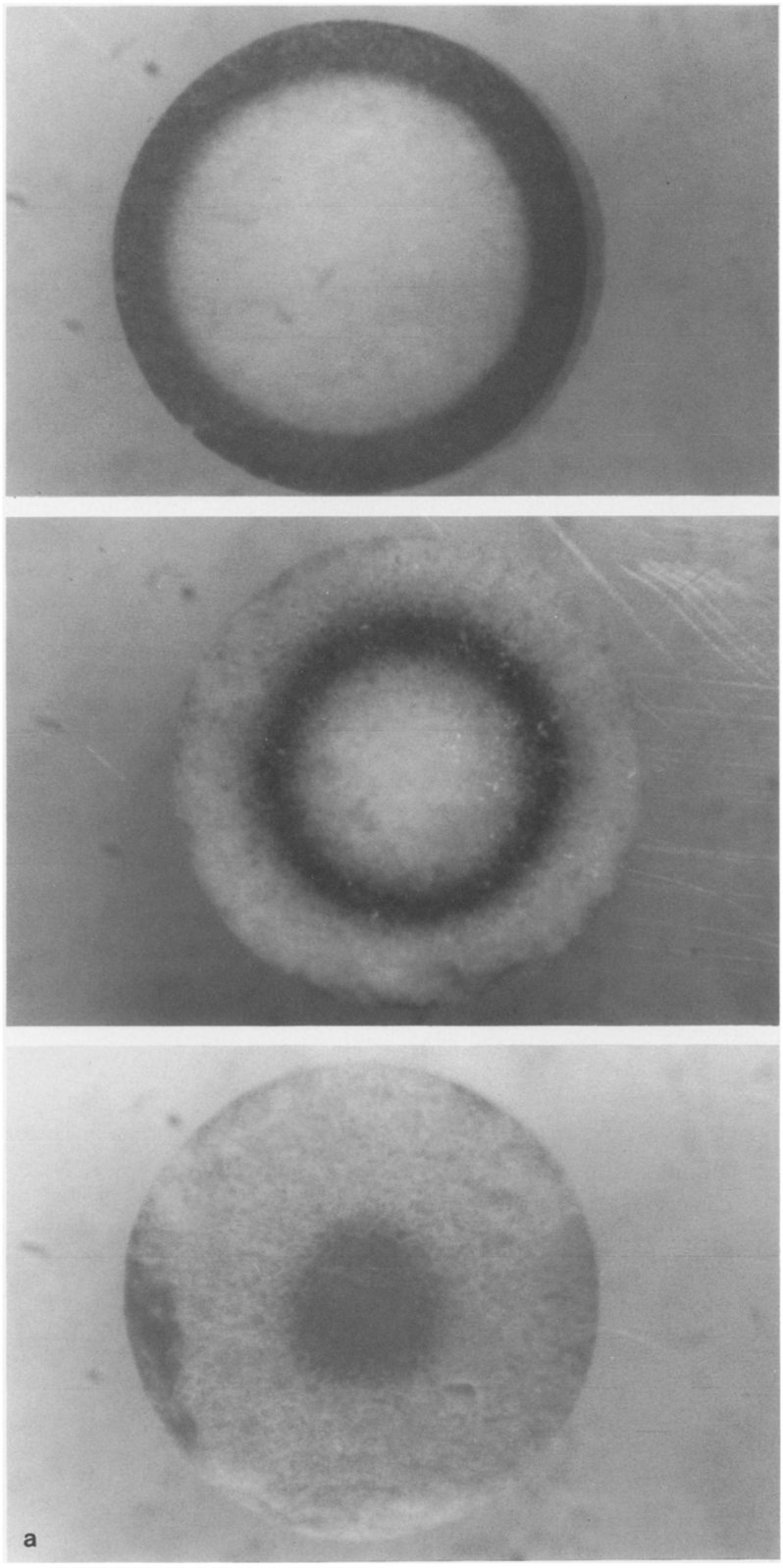

FIG. 2. Cross sections of 3-mm-diameter γ-Al_2O_3 cylindrical pellets with egg shell, egg white, and egg yolk Pt (a) and Ag (b) catalyst distribution. Total metal load: 0.3 wt% Pt and 3.0 wt% Ag.

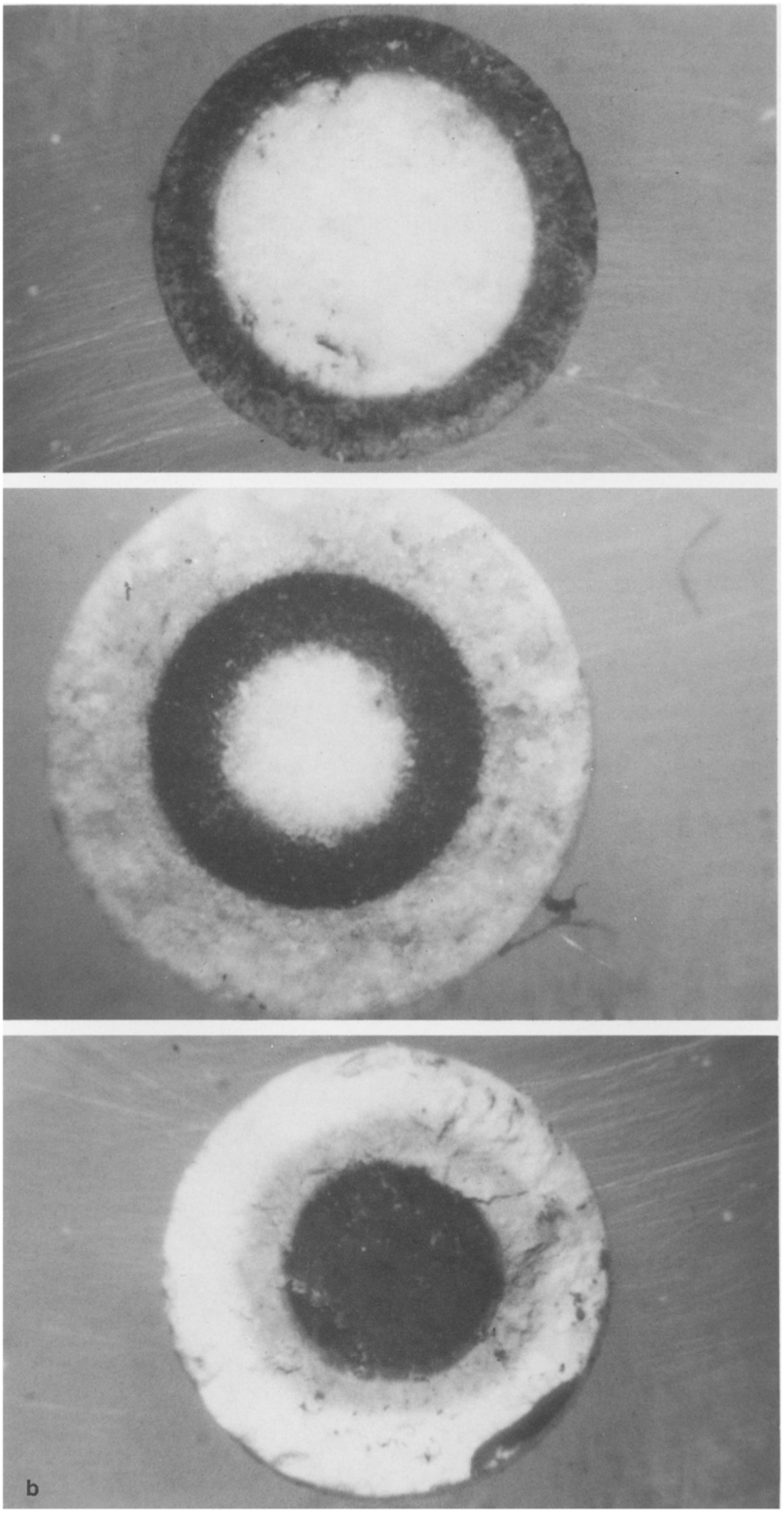

FIG. 2—*Continued*

35). The procedure usually involves partial impregnation and use of site-blocking agents in the impregnation solution. The Pt/γ-Al_2O_3 and Ag/γ-Al_2O_3 pellets shown in Fig. 2 were prepared by using citric acid as the site-blocking agent in the impregnating H_2PtCl_6 and $AgNO_3$ solutions, respectively. By varying the citric acid concentration in the solution and the impregnating time, the location and the width of the active catalyst zone can be controlled. Experimental preparation details will appear elsewhere (*36*).

APPLICATIONS AND DISCUSSION

In this section, the results of the previous analysis are applied to determine the optimal catalyst activity profile for two triangular reaction networks of significant catalystic interest, i.e., epoxidation of ethylene and epoxidation of propylene on Ag catalysts. The former system corresponds to a well-established industrial process, the catalytic mechanism of which is still under intensive study (*30–33*). The latter system is not of industrial importance, because of the very low intrinsic selectivity of Ag for propylene oxide formation, i.e., typically less than 4% (*29*), which is well below the selectivity obtained in the commercial Oxirane process (*37*). However, this system is presented as an example of how an optimally impregnated pellet can lead to positive selectivity, i.e., desired product formation, whereas a uniformly impregnated pellet yields negative selectivity, i.e., net consumption of the desired product.

Ethylene Epoxidation on Ag

The kinetics of this triangular reaction network have been studied extensively because of its industrial importance in the production of ethylene oxide. The effect of nonuniform catalyst distibution on global catalyst pellet selectivity has been explored in two previous studies (*17, 20*). To apply the analysis of the previous sections, the network can be written formally as

TABLE 3

Ethylene Epoxidation on Ag: Dimensionless Rate Expressions and Parameter Values Used in Computations

$$\varphi_1(u_1, \theta) = \frac{(1 + \sigma_1)u_1 \exp[\gamma_1(1 - 1/\theta)] \exp[-\gamma_1^*(1 - 1/\theta)]}{1 + \sigma_1 u_1 \exp[-\gamma_1^*(1 - 1/\theta)]}$$

$$\varphi_2(u_1, \theta) = \frac{(1 + \sigma_1)u_1 \exp[\gamma_2(1 - 1/\theta)] \exp[-\gamma_1^*(1 - 1/\theta)]}{1 + \sigma_1 u_1 \exp[-\gamma_1^*(1 - 1/\theta)]}$$

$$\varphi_2(u_1, \theta) = \frac{(1 + \sigma_2^2)(\xi u_2)^2 \exp[\gamma_3(1 - 1/\theta)] \exp[-2\gamma_2^*(1 - 1/\theta)]}{1 + \sigma_2^2(\xi u_2)^2 \exp[-2\gamma_2^*(1 - 1/\theta)]}$$

$\sigma_1 = 8.7 \times 10^{-4} \exp(\gamma_1^*) P_1^o$	$(-\Delta H_2) = 1324$ kJ/mol C_2H_4
$\sigma_2 = 5.7 \times 10^{-3} \exp(\gamma_2^*) P_1^o$	$(-\Delta H_3) = 1203$ kJ/mol C_2H_4O
$\gamma_1 = 7300/T_0$	$\xi = D_{e,1}/D_{e,2}$
$\gamma_2 = 11{,}100/T_0$	$D_{e,1} = 2.9 \times 10^{-7}$ m²/s
$\gamma_3 = 10{,}200/T_0$	$D_{e,2} = 2.3 \times 10^{-7}$ m²/s
$\gamma_1^* = 5800/T_0$	$K_e = 8.4 \times 10^{-2}$ W/(m K)
$\gamma_2^* = 5300/T_0$	Catalyst dispersion: 0.1
	$g_0 = 7.3$ kg/m³
	$R = 3$ mm

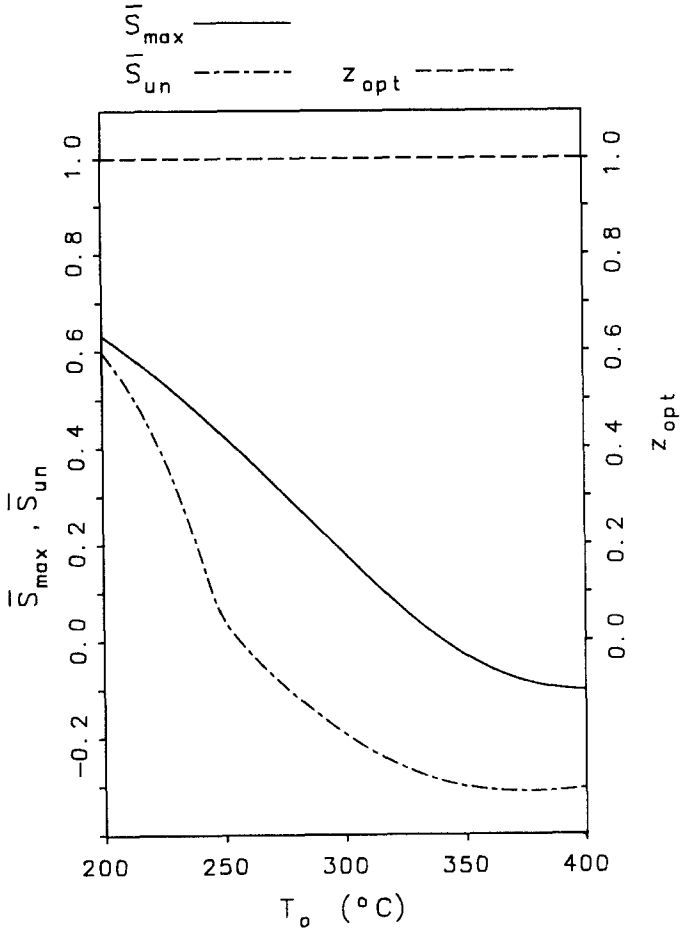

FIG. 3. Effect of ambient temprature on $\bar{S}_{max}$ and $\bar{S}_{un}$ for ethylene epoxidation on Ag in excess O_2: P = 1 bar, y_{Et} = 0.05, y_{EtO} = 0.05, z_{opt} = 1.

$$C_2H_4 + 3O_2 \xrightarrow{1} C_2H_4O + \tfrac{5}{2}O_2$$
$$\text{2: } C_2H_4 + 3O_2 \rightarrow 2CO_2 + 2H_2O$$
$$\text{3: } C_2H_4O + \tfrac{5}{2}O_2 \rightarrow 2CO_2 + 2H_2O \qquad (31)$$

Consequently, the stoichiometric coefficients a_{ij} take the values $a_{11} = 1$, $a_{12} = 0$, $a_{13} = 0$, $a_{21} = 0$, $a_{22} = 1$, $a_{23} = 0$, $a_{31} = 3$, $a_{32} = \frac{5}{2}$, $a_{33} = 0$, where $i = 1, 2, 3$ denotes C_2H_4, C_2H_4O, and O_2, respectively. Two invariants exist:

$$u_3 = u_3^o - 3(1 - u_1) - (\tfrac{5}{2})(u_2^o - u_2) \qquad (32)$$

$$\theta = 1 + \beta_2(1 - u_1) + (\beta_2 - \beta_1)(u_2^o - u_2). \qquad (33)$$

Table 3 lists the kinetic, thermodynamic, and transport parameter values used in the computations. The kinetic expressions are those given by Stoukides and Vayenas (*26–29*) and are applicable for fuel-lean gaseous compositions. However, the exact form of kinetic parameters used is expected to have no significant effect on the optimal catalyst location z_{opt} of this reaction system, be-

TABLE 4

Propylene Epoxidation on Ag: Dimensionless Rate Expressions and Parameter Values Used in Computations

$$\varphi_1(u_1, \theta) = \frac{(1 + \sigma_1)u_1 \exp[\gamma_1(1 - 1/\theta)] \exp[-\gamma_1^*(1 - 1/\theta)]}{1 + \sigma_1 u_1 \exp[-\gamma_1^*(1 - 1/\theta)]}$$

$$\varphi_2(u_1, \theta) = \frac{(1 + \sigma_1)u_1 \exp[\gamma_2(1 - 1/\theta)] \exp[-\gamma_1^*(1 - 1/\theta)]}{1 + \sigma_1 u_1 \exp[-\gamma_1^*(1 - 1/\theta)]}$$

$$\varphi_2(u_1, \theta) = \frac{(1 + \sigma_2)(\xi u_2) \exp[\gamma_3(1 - 1/\theta)] \exp[-\gamma_2^*(1 - 1/\theta)]}{1 + \sigma_2(\xi u_2) \exp[-\gamma_2^*(1 - 1/\theta)]}$$

$\sigma_1 = 1.2 \times 10^{-4} \exp(\gamma_1^*) P_1^\circ$	$(-\Delta H_1) = 113.5$ kJ/mol C_3H_6
$\sigma_2 = 1 \times 10^{-2} \exp(\gamma_2^*) P_1^\circ$	$(-\Delta H_2) = 1929$ kJ/mol C_3H_6O
$\gamma_1 = 11{,}000/T_0$	$\xi = D_{e,1}/D_{e,2}$
$\gamma_2 = 9500/T_0$	$D_{e,1} = 2.6 \times 10^{-7}$ m²/s
$\gamma_3 = 9500/T_0$	$D_{e,2} = 2.3 \times 10^{-7}$ m²/s
$\gamma_1^* = 7500/T_0$	$K_e = 8.4 \times 10^{-2}$ W/(m K)
$\gamma_2^* = 5250/T_0$	Catalyst dispersion: 0.1
	$g_0 = 7.3$ kg/m³
	$R = 3$ mm

cause the activation energy E_1 of the desired reaction of this system is well known to be smaller than E_2. Consequently, intraparticle temperature gradients can have only a detrimental effect on global selectivity. Since practically all previous kinetic studies of this reaction system have reported positive- or zero-order dependence of the rates on the reactants, it follows that intraparticle concentration gradients will also have an adverse effect on global selectivity. It is not surprising then that application of the results of Table 1 gives $z_{opt} = 1$ for practically all conditions for this reaction system; i.e., the egg shell distribution is optimal. Figure 3 shows the effect of ambient temperature on the maximum global selectivity and on that obtained with uniform catalyst distribution. The difference between $\bar{S}_{max}$ and $\bar{S}_{un}$ increases with increasing temperature. The result that $z_{opt} = 1$ is in agreement with the numerical results of Johnson and Verykios (*17*), who showed that global selectivity increases when the catalyst concentration increases with distance from the center of the pellet.

Propylene Epoxidation on Ag

The kinetics of this network have been studied in detail (*28, 29*) and the resulting rate expressions, which are valid for fuel-lean gaseous compositions (*29*), are given in Table 4 in dimensionless form. The network can be written formally as follows:

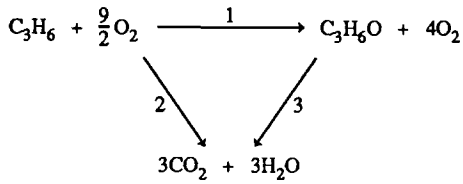

(34)

Consequently, the stoichiometric coefficients a_{ij} have the values $a_{11} = 1$, $a_{12} = 0$, $a_{13} = 0$, $a_{21} = 0$, $a_{22} = 1$, $a_{23} = 0$, $a_{31} = \frac{9}{2}$, $a_{32} = 4$, $a_{33} = 0$, where $i = 1, 2, 3$ denotes

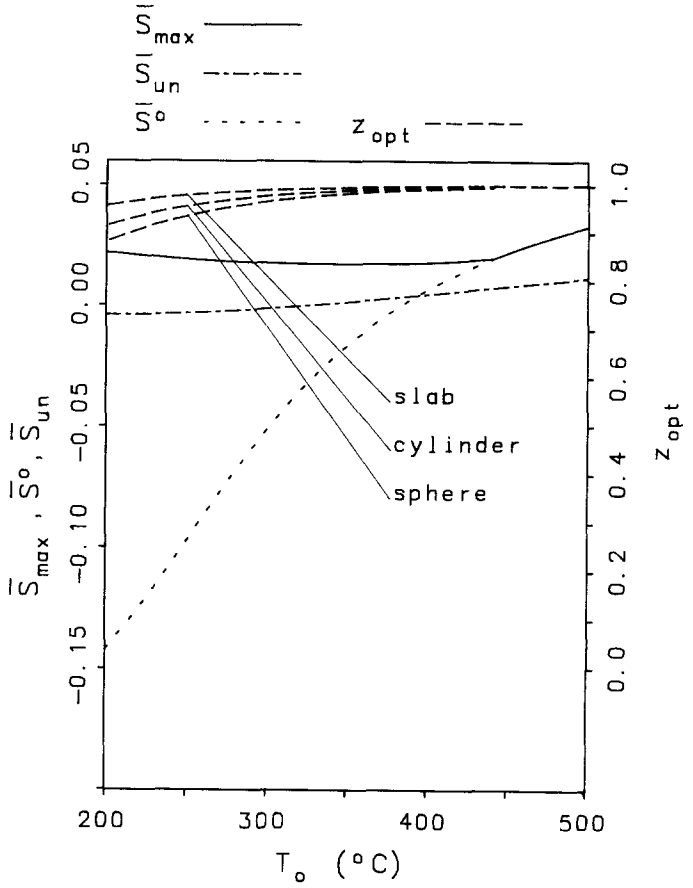

FIG. 4. Effect of ambient temperature on optimal catalyst location z_{opt} and on global pellet selectivity obtained with optimal ($\bar{S}_{max}$), egg shell ($\bar{S}^o$), and uniform ($\bar{S}_{un}$) catalyst distribution in excess O_2: $P = 7$ bar, $y_{Pr} = 0.2$, $y_{PrO} = 0.001$.

C_3H_6, C_3H_6O, and O_2, respectively. The two invariants are

$$u_3 = u_3^o - (\tfrac{9}{2})(1 - u_1) - 4(u_2^o - u_2) \quad (35)$$

$$\theta = 1 + \beta_2(1 - u_1) + (\beta_2 - \beta_1)(u_2^o - u_2). \quad (36)$$

The kinetic differences between this reaction network and ethylene epoxidation have been discussed (*29*). The main difference is the much higher turnover rate of direct propylene oxidation to CO_2 in relation to the turnover rate of epoxidation. Another difference is that the activation energy E_1 of the desired reaction is slightly higher than E_2 and E_3 (*29*) (Table 4). As a result, the intrinsic selectivity $\bar{S}^o$ as well as the selectivity $\bar{S}_{un}$ obtained in uniformly activated pellets increase with increasing temperature up to 500°C, as shown in Fig. 4. The same figure shows that at temperatures above 430°C, $z_{opt} = 1$; i.e., the egg shell distribution is optimal. However, at lower temperatures the optimal catalyst location is inside the pellet and this can maintain positive global selectivities where, as shown in the same figure, both $\bar{S}^o$ and $\bar{S}_{un}$ are negative. Under these conditions, a uniformly or egg shell impregnated catalyst would lead to net consumption of propylene oxide, whereas an optimally impreg-

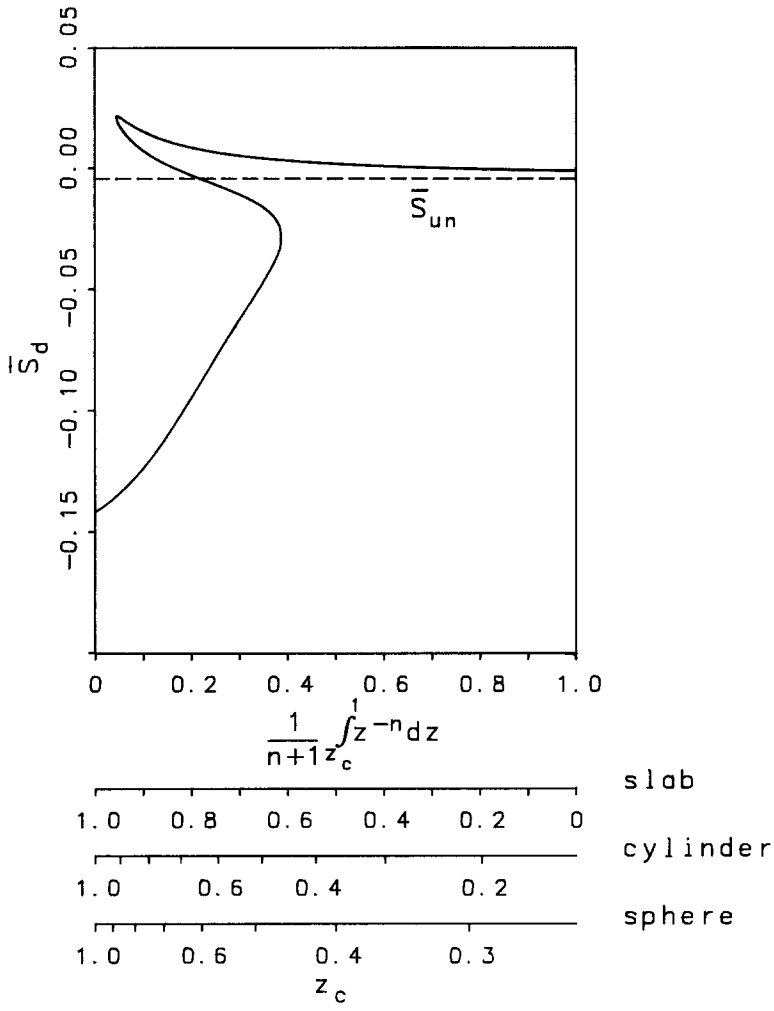

FIG. 5. Effect of catalyst location z_c on global pellet selectivity $\bar{S}_d$ obtained with a Dirac-type distribution and comparison with $\bar{S}_{un}$: $P = 7$ bar, $T_0 = 200°C$, $y_{Pr} = 0.2$, $y_{PrO} = 0.001$.

nated catalyst would lead to net production of propylene oxide.

Figure 5 shows the effect of catalyst location on the selectivity $\bar{S}_d$ obtained with a Dirac-type distribution under the conditions of Fig. 4 and $T_0 = 200°C$. The same figure compares $\bar{S}_d$ with $\bar{S}_{un} = -0.004$ and $\bar{S}^o = -0.142$ and shows that a Dirac-type impregnated pellet leads to steady-state multiplicity with the ignited branch exhibiting positive selectivity, whereas both $\bar{S}_{un}$ and $\bar{S}^o$ are negative.

The effect of ambient mole fraction of propylene oxide y_{PrO} on z_{opt} and $\bar{S}^o$, $\bar{S}_{un}$, and $\bar{S}_{max}$ is shown in Fig. 6. Increasing y_{PrO} causes a very pronounced decrease in $\bar{S}^o$ and $\bar{S}_{un}$ and only a moderate one in $\bar{S}_{max}$. It can be seen that the advantage of optimally impregnated pellets becomes more pronounced at higher values of y_{PrO}, i.e., at higher ambient propylene conversion.

SUMMARY

Rigorous analytical expressions have been found for the optimal catalyst distribution profile in porous pellets for maximiza-

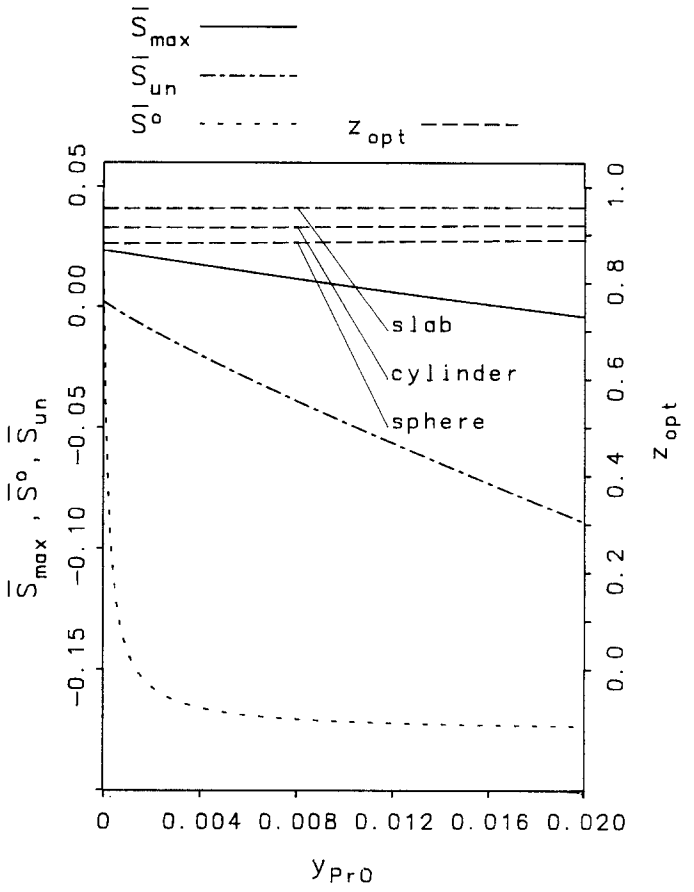

FIG. 6. Effect of ambient propylene oxide mole fraction on optimal catalyst location z_{opt} and on global pellet selectivity obtained with optimal ($\bar{S}_{max}$), egg shell ($\bar{S}^o$), and uniform ($\bar{S}_{un}$) catalyst distribution in excess O_2: P = 7 bar, T_0 = 200°C, y_{Pr} = 0.2.

tion of global selectivity. The expressions are applicable to cases of parallel, consecutive, or triangular reaction networks with arbitrary kinetics and arbitrary numbers of reactants and products. Flat, cylindrical, or spherical pellets can be isothermal or nonisothermal. The results are summarized in Table 1 and show that the optimal catalyst distribution corresponds to deposition of the active component in a thin layer located at a distance z_{opt} from the center of the pellet.

Application of these theoretical results to the epoxidation of C_2H_4 and of C_3H_6 shows that optimally impregnated pellets can give significantly higher global selectivity than uniformly impregnated pellets.

The preparation of pellets with near-optimal catalyst profiles does not appear to pose difficult experimental problems. Experimental verification of theoretical predictions will be necessary before optimally impregnated catalyst pellets can be considered for selectivity maximization in industrial applications.

APPENDIX: NOTATION

A_i	ith chemical species
a_{ij}	Stoichiometric coefficient of the ith chemical species in the jth reaction network node
c_i	Concentration of species A_i

$D_{e,i}$ Effective diffusion coefficient of species A_i
E_j Activation energy of jth reaction
f_j Reaction rate expression of jth reaction
g, g_0 Local and volume-averaged catalyst density
h_1, h_2 Functions defined in Eqs. (20) and (21)
$(-\Delta H_j)$ Heat of jth reaction
K_e Effective thermal conductivity
n Integer characteristic of pellet geometry: $n = 0$ for infinite slab, $n = 1$ for infinite cylinder; $n = 2$ for sphere
P Pressure
R Characteristic pellet dimension; thickness or half-thickness of slab exposed to reactants on one or both sides, respectively ($n = 0$); radius of cylinder or sphere ($n = 1, 2$)
$\bar{S}$ Global selectivity
$\bar{S}_d$ Global selectivity obtained with a Dirac-type catalyst distribution
$\bar{S}_{max}$ Maximum global selectivity
T Temperature
T_0 Temperature at pellet surface
u_i Dimensionless concentration of species i, $c_i D_{e,i}/(c_1^o D_{e,1})$
V_p Pellet volume
x Distance from center of pellet
y Mole fraction
z Dimensionless distance from center of pellet, x/R

Greek Letters

α Activity distribution function
β_j dimensionless heat of reaction, $(-\Delta H_j)c_1^o D_{e,1}/(K_e T_0)$
γ_j Dimensionless activation energy, $E_j/(RT_0)$
γ_1^*, γ_2^* Dimensionless heats of adsorption, Tables 3 and 4
δ Dirac delta function
θ Dimensionless temperature, T/T_0
κ Φ_2^2/Φ_1^2
λ Φ_3^2/Φ_1^2
Λ_{cp} Parameter defined in Table 2
ξ $D_{e,1}/D_{e,2}$
σ_1, σ_2 Dimensionless adsorption equilibrium constants, Tables 3 and 4
Φ_j Thiele modulus, $\{g_0 R^2 f_j(c_1^o, \ldots, c_1^o, T_0)/[(n+1)D_{e,1}c_1^o]\}^{1/2}$
φ_j Dimensionless reaction rate expressions, $f_j(c_1, \ldots, c_m, T)/f_j(c_1^o, \ldots, c_1^o, T_0)$
$\hat{\varphi}_j$ Equivalent reaction rate expressions resulting from elimination of u_i ($i = 3, \ldots, m$) and θ from φ_j by use of Eqs. (13) and (15)
φ_j^* Function in reaction rate expressions, Eq. (30)
Ω Dimensionless parameter defined in Table 1

Subscripts

Et Denotes quantity corresponding to ethylene
EtO Denotes quantity corresponding to ethylene oxide
Pr Denotes quantity corresponding to propylene
PrO Denotes quantity corresponding to propylene oxide
opt Denotes value corresponding to the optimal catalyst distribution
un Denotes value corresponding to the uniform distribution

Superscripts

o Denotes conditions at the pellet surface

ACKNOWLEDGMENTS

We thank Mr. P. Tsiakaras of our Institute for preparing the Pt/γ-Al_2O_3 and Ag/γ-Al_2O_3 pellets shown in Fig. 2 and the Hellenic Refineries (ELDA) for financial support. We also thank one of our reviewers for some thoughtful suggestions.

REFERENCES

1. Shadman-Yazdi, F., and Petersen, E. E., *Chem. Eng. Sci.* **27,** 227 (1972).
2. Wei, J., and Becker, E. R., *J. Catal.* **46,** 372 (1977).

3. Hegedus, L. L., and Summers, J. C., *J. Catal.* **48,** 345 (1977).
4. Summers, J. C., and Hegedus, L. L., *J. Catal.* **51,** 185 (1978).
5. Hegedus, L. L., Summers, J. C., Schlatter, J. C., and Baron, K., *J. Catal.* **56,** 321 (1979).
6. Morbidelli, M., Servida, A., and Varma, A., *Ind. Eng. Chem. Fundam.* **21,** 278 (1982).
7. Morbidelli, M., and Varma, A., *Ind. Eng. Chem. Fundam.* **21,** 284 (1982).
8. Morbidelli, M., Servida, A., Carrà, S., and Varma, A., *Ind. Eng. Chem. Fundam.* **24,** 116 (1985).
9. Vayenas, C. G., and Pavlou, S., *Chem. Eng. Sci.* **42,** 2633 (1987).
10. Chemburkar, R., Morbidelli, M., and Varma, A., *Chem. Eng. Sci.* **42,** 2621 (1987).
11. Dougherty, R. C., and Verykios, X. E., *Catal. Rev.-Sci. Eng.* **29,** 101 (1987).
12. Vayenas, C. G., and Verykios, X. E., *in* "Handbook of Heat and Mass Transfer" (N. P. Cheremisinoff, Ed.), Vol. 3, pp. 135–181. Gulf Publishers, 1988.
13. Wu, H., Yuan, Q., and Zhu, B., *Ind. Eng. Chem. Res.* **27,** 1169 (1988).
14. Lee, C. K., and Varma, A., *Chem. Eng. Sci.* **43,** 1995 (1988).
15. Ernst, W. R., and Daugherty, D. J., *AIChE J.* **24,** 935 (1978).
16. Juang, H. D., and Weng, H. S., *Ind. Eng. Chem. Fundam.* **22,** 224 (1983).
17. Johnson, D. L., and Verykios, X. E., *J. Catal.* **79,** 156 (1983).
18. Cukierman, A. L., Laborde, M. A., and Lemcoff, N. O., *Chem. Eng. Sci.* **38,** 1977 (1983).
19. Dadyburjor, D. B., *Ind. Eng. Chem. Fundam.* **24,** 16 (1985).
20. Morbidelli, M., Servida, A., Paludetto, R., and Carrà, S., *J. Catal.* **87,** 116 (1984).
21. Dougherty, R. C., and Verykios, X. E., *AIChE J.* **32,** 1858 (1987).
22. Vayenas, C. G., and Pavlou, S., *Chem. Eng. Sci.* **42,** 1655 (1987).
23. Vayenas, C. G., and Pavlou, S., *Chem. Eng. Sci.* **43,** 2729 (1988).
24. Vayenas, C. G., Pavlou, S., and Pappas, A., *Chem. Eng. Sci.* **44,** 133 (1989).
25. Verykios X. E., Stein, F. P., and Coughlin, R. W., *Catal. Rev.-Sci. Eng.* **22,** 197 (1980).
26. Stoukides, M., and Vayenas, C. G., *J. Catal.* **64,** 18 (1980).
27. Stoukides, M., and Vayenas, C. G., *J. Catal.* **69,** 18 (1981).
28. Stoukides, M., and Vayenas, C. G., *J. Catal.* **74,** 266 (1982).
29. Stoukides, M., and Vayenas, C. G., *J. Catal.* **82,** 45 (1983).
30. Campbell, C. T., and Koel, B. E., *J. Catal.* **92,** 272 (1985).
31. Grant, R. B., and Lambert, R. M., *J. Catal.* **92,** 364 (1985).
32. Tan, S. A., Grant, R. B., and Lambert, R. M., *J. Catal.* **106,** 54 (1987).
33. Boghosian, S., Bebelis, S., Vayenas, C. G., and Papatheodorou, G. N., *J. Catal.* **117,** 561 (1989).
34. Kotter, M., and Riekert, L., *Chem. Eng. Fundam.* **2,** 19 (1983).
35. Kotter, M., and Riekert, L., *Chem. Eng. Fundam.* **2,** 21 (1983).
36. Tsiakaras, P., Verykios, X. E., and Vayenas, C. G., in preparation.
37. Kuhn, W., *Chem. Eng. Progr.* **76**(1), 53 (1980).